

Supporting Information

High Performance Graphene Embedded Rubber Composites

Sung Ho Song^{1*}, Jung Mo Kim², Kwang Hyun Park³, Dong Ju Lee², O-Seok Kwon⁴, Jin Kim²,
Hyewon Yoon², Xianjue Chen¹

¹ Institute of Basic Science (IBS) Center for Multidimensional Carbon Materials (CMCM)
(located at the Ulsan National Institute of Science and Technology Campus), Ulsan National
Institute of Science and Technology (UNIST), Ulsan 689-798, Republic of Korea

² Department of Materials Science and Engineering and Graphene Research Center of KI for the
NanoCentury, Korea Advanced Institute of Science and Technology (KAIST), Daejeon 305-701,
Republic of Korea.

³ School of Energy and Chemical Engineering, KIER-UNIST Advanced Center for Energy, Low
Dimensional Carbon Materials Center, Ulsan National Institute of Science and Technology
(UNIST), Ulsan 689-798, Republic of Korea

⁴ NEXEN Tire Corporation R&D Center, 30, Yusan-Dong, Yangsan-Si, Kyungnam, 626-230,
Republic of Korea

E-mail: shsong805@kaist.ac.kr

S1. Experimental

S1.1. Materials

S1.2. Preparation of Graphene oxide

S1.3. Preparation of Graphene (*l*-GFs)

S1.4. Preparation of Rubber composites

S1.5. equipment & techniques

S2. Characterization

S2.1. AFM image of *l*-GFs according to the size and thickness

S2.2. AFM image of *l*-GFs

S2.3. HRTEM images of *l*-GFs

S2.4. XPS analysis of GO and *l*-GFs

S2.5. FT-IR analysis of Graphite, GO and *l*-GFs

S2.6. Thermalgravimetric analysis (TGA) of Graphite, GO and *l*-GFs

S2.7. SEM images of Rubber composite

Table S1. Formation of Rubber composites

Table S2. Curing properties of Rubber composites

S1. Experimental

S1.1. Materials

Graphite powder was purchased from Bay Carbon, Inc. (SP-1 graphite powder). The matrix material was Styrene Butadiene Rubber (SBR) from Kumho petrochem Co. Ltd., Korea. The SBR 1500 was consisted of 23% styrene and 77% butadiene. The carbon black (N-330) which was filled with SBR compounds was made of OCI Co. Ltd., Korea, and N-tert-butylbenzothiazole sulfonamide (TBBS) with a role of curatives was purchased from ShangdongShanxian Co. Ktd., China. Zinc oxide (ZnO), stearic acid (S/A), sulfur, oleic acid were purchased from standard local suppliers.

S1.2. Preparation of Graphene Oxide

Graphene oxide was obtained from SP-1 graphite (Bay Carbon) using the modified Hummers method.^[1] The oxidation product was purified by rinsing with a 10% HCl solution, repeatedly washing with copious amounts of Di-water, and filtering through an anodisc aluminium oxide (AAO, 0.2 μm pores, Whatman) filter. The filtered material was dried under vacuum (80 °C, 12 h).

S1.3. Preparation of *l*-GFs and Dispersion

Worm like expanded graphite (WEG) is a well-known material usually produced from various intercalation compounds submitted to a thermal shock. In this work, WEG was prepared by a conventional acid process combining with thermal exfoliation.^[2] First, GICs were synthesized from natural graphite (with a purity of 99 wt%). For the intercalation, pristine natural graphite flakes were mixed with a mixture (20 : 1 by volume) of concentrated sulfuric acid (98 wt.%) and hydrogen peroxide (30 wt.%). The obtained mixture was then stirred for about 1 h and then washed with deionized water until the pH level reached. After drying at 100 °C for 24 h, the expandable graphite was obtained. When GICs were heated at a certain temperature (200 ~ 1000

°C), the decomposition of the intercalating acid leads to a sudden and dramatic increase in the dimension perpendicular to the graphene sheets. In this experiment, the expansion process was carried out at 900 °C by rapidly heating the GIC sample for 20 s.

The obtained WEG was subjected to a final exfoliation to obtain monolayer or a few layers of graphene sheets (*l*-GFs) by ultrasonication and centrifugation of a 1-methyl-2-pyrrolidinone (NMP) suspension (0.1 mg/mL) of the sample. The *l*-GFs were filtered and washed with de-ionized (DI) water using a 0.1 micron Anodisc filter to remove the salts and residual solvent. The product was dried under 100 °C in a furnace. To measure the yield of *l*-GFs, the dispersed graphene flakes were filtered out by using an anodisc aluminium oxide (AAO, 0.2 µm pores, Whatman) filter and washed with warm distilled water (pH2). We carefully avoid sedimented graphene flake during filtrating process. After drying for 24 h, the yield of graphene flakes was discreetly measured on the basis of weight change. The yield of *l*-GFs was estimated to be 30 wt%. The *l*-GFs (10 mg) were dispersed in 30ml of various solvents (acetone, DMF, THF, ethanol, pyridine, methanol, water) with sonication for 3 hours. All solvents were purchased from Sigma - Aldrich. After 2 weeks, absorbance (A) was measured for each suspension. After making a baseline with each pure solvent, a quartz cell was filled with the *l*-GF suspension and pure solvent with different concentrations, such as 1:2, 2:1, and 3:0.

S1.4. Preparation of Rubber composites

The carbon materials/SBR composites were prepared by following standard procedures. First, the SBR latex (20phr) with 5 phr (parts per hundred rubber by weight) of carbon black, graphite, GO, and Graphene (*l*-GFs) were mixed by vigorous stirring for 24 h, respectively. During coagulation, butadiene-styrene-vinyl-pyridine rubber (VPR) was added to a small loading. The VPR prevents the aggregation of *l*-GFs and acts as an interface-bridge between *l*-GFs and SBR.

The carbon nanomaterials/SBR emulsion was then coagulated by a 1.0 phr sulfuric acid solution. The coagulated composites were washed with water until the pH of the filtered water reached 6 ~ 7 and then dried in an oven at 50 °C for 24 h. And then, the SBR 80 phr and carbon materials (5 phr)/SBR emulsion (20 phr) were mixed with 50 phr carbon black in Banbury mixer at a rotor speed of 60 rpm for mater batches. The additives and vulcanization agents were added at the end so that curing process of the mixture could be started. The compounds were placed in the aluminum mold and cured at 160 °C for T_{90} by rheometer under pressure. The formulations of the carbon materials/SBR composites are summarized in Table S1.

S1.5. equipment & techniques

Morphology of *l*-GFs was analysed using an atomic force microscope (AFM, SPA400, SII, Japan) in tapping mode under ambient conditions. X-ray photoelectron spectroscopy (XPS, Sigma Probe, AlK α), transmission electron microscopy (TEM, Tecnai G2 F30) analyses were conducted. TEM samples were prepared by drying a droplet of the *l*-GFs suspensions on a carbon grid. **A thermogravimetric analysis (TGA, NETZSCH TG 209 F3 Tarsus, Germany) was performed at a heating rate of 10 °C/min under Ar atmosphere.** Raman spectra were obtained from 1200 to 3000 cm⁻¹ using a Raman spectrometer (LabRAM HR UV/Vis/NIR, excitation at 514nm). The FT-IR spectrum was measured using a FT-IR-4100 type-A FT-IR spectrometer with pure KBr as the background from 1000 and 3000 cm⁻¹. The thermal conductivity was measured with a LFA 447. Thermal imaging camera (AX8, MDS Technology Co., Ltd) was obtained Temperature curves of SBR composites with GO and *l*-GFs according to time. Scanning electron microscopy (SEM, JEOL JSM-6490LV) was used to observe the morphology of the fractured surface of Rubber composites. The specimens were fractured in liquid nitrogen and the cross surface of samples were coated by gold using a sputtering process. Curing

characteristics were measured over 30 min periods at 160 °C using a moving-die rheometer (DRM-100(LP-171)). Tensile tests were carried out in an Instron tensile machine (Instron Co., UK) at crosshead speed of 300 mm/min. The dumbbell shape samples were 100 mm in thickness and 5 mm in width. At least four tests were carried out for each case.

S2. Characterization

S2.1. AFM images of *l*-GFs according to the size and thickness

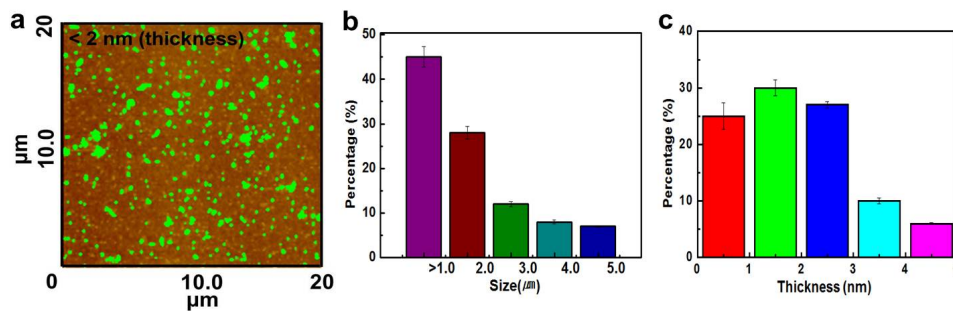


Figure S2.1. a. Atomic force microscopy (AFM) images of *l*-GFs on silicon oxide. b. Statistical analysis a histogram plotted as a function of size. c. Statistical analysis a histogram plotted as a function of thickness.

Additional AFM images are shown Figure S2.1. Their dominant sizes of *l*-GFs are mainly distributed under 1 μm (~44.8 %), and their topological thickness fall between 1.0 ~ 2.0 nm (~30.0 %) in Figure S2.1.

S2.2. AFM image of *l*-GFs

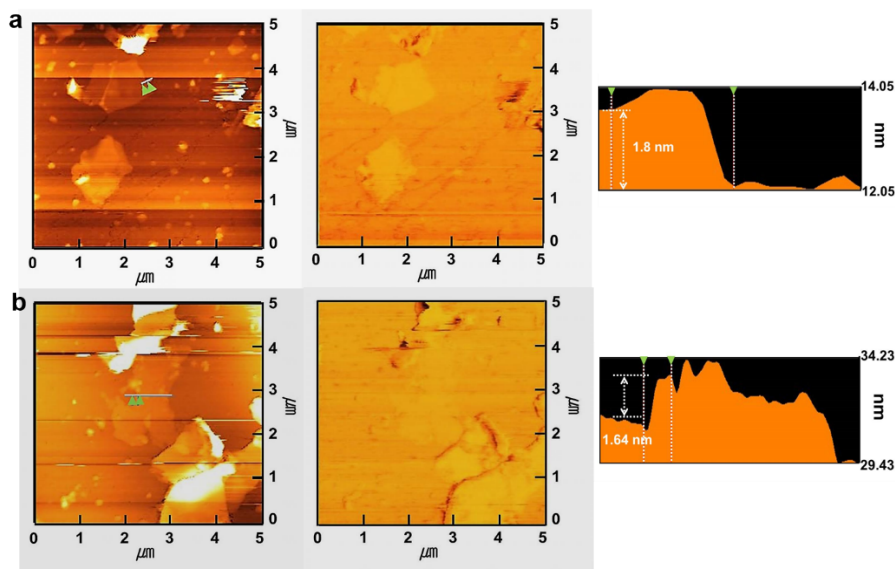


Figure S2.2. AFM image of *l*-GFs

Figure S2.2 shows the atomic force microscopy (AFM) images of *l*-GFs. The samples of AFM analysis were prepared by depositing on the silicon oxide substrates and dried under vacuum at 100 °C. The thickness of *l*-GFs was determined to be ~ 1.7 nm, which corresponds to the height of a mono or bilayer graphene.

S2.3. HRTEM images of *l*-GFs

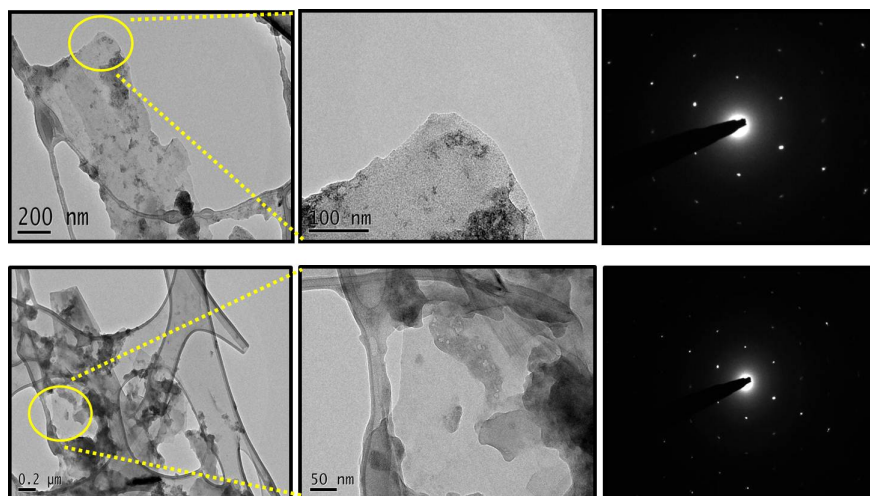


Figure S2.3. HRTEM images of *l*-GFs on TEM grids from the dispersion, and SAED pattern of *l*-GFs at 200kV.

Figure S2.3 shows HRTEM images of a single layer *l*-GFs produced by our system, and the single layer *l*-GFs retains the crystallite structure with clear diffraction patterns. The hexagonal pattern from the SAED data shows that the crystallinity of the *l*-GFs is not degraded after the treatment.

S2.4. XPS analysis of GO and *l*-GFs

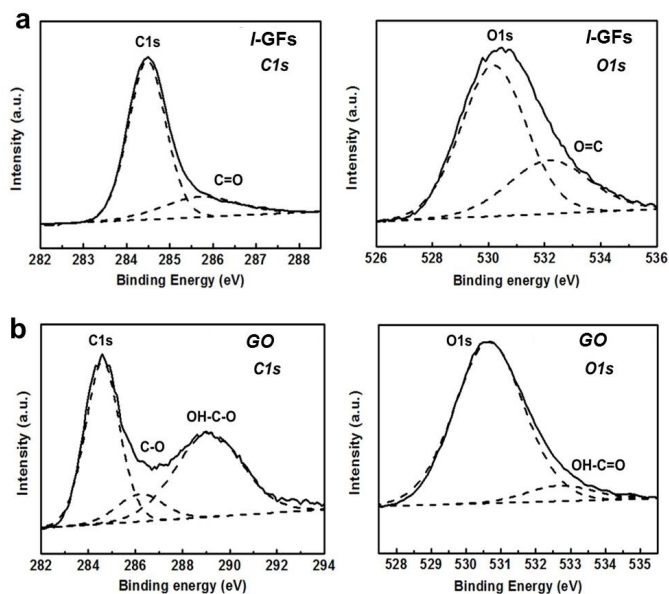


Figure S2.4. a. C1s XPS spectra and O1s XPS spectra of the *l*-GFs on silicon oxide. b. C1s XPS spectra and O1s XPS spectra of the GO on silicon oxide.

In Figure S2.4, detailed compositional analysis of GO and *l*-GFs were carried out, and the C1s XPS spectrum of *l*-GFs consisted of the C-C bond (284.5 eV) of sp² carbon, C=O groups (288.2 eV) of the carbonyl group, and the OH-C=O bond (290.1 eV) of carboxylic carbon in Figure 2a. Also, the C1s XPS spectrum of GO (Figure S2b) indicates the presence of four types of carbon bond: C-C (284.5 eV), C-O (286.6 eV), C=O (288.2 eV) and OH-C=O (289.1 eV). Information provided by analysis of O1s spectra can complement the information provided by analysis of C1s spectra, and the O1s spectrum shows O-O (530.5 eV), C=O (532.5 eV) and OH-C=O (533.5eV).

S2.5. FT-IR analysis of Graphite, GO and *l*-GFs

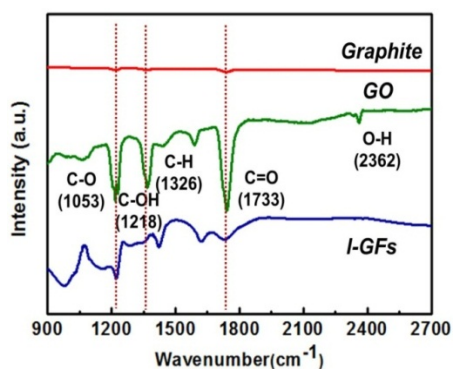


Figure S2.5. FT-IR analysis of Graphite, GO and *l*-GFs

In the FT-IR spectra of both GO and *l*-GFs, three characteristic peaks related to C-O stretching, C-OH stretching, and C=O stretching in the carboxylic acid and carbonyl moieties are seen in Figure S2.5. The peaks observed in GO and *l*-GFs do not appear in the spectrum of the graphite.

S2.6. Thermalgravimetric analysis (TGA) of Graphite, GO and *l*-GFs

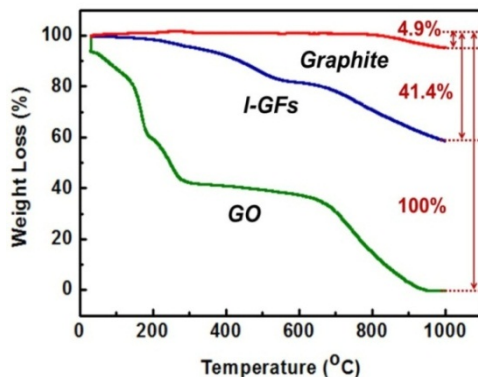


Figure S2.6. TGA of Graphite, GO and *l*-GFs

Figure S2.6 displays the TGA that show weight loss as a function of temperature. The GO sample showed significant weight loss with an onset temperature. The *l*-GFs showed much higher stability because of de-oxygenation of *l*-GFs. When all the samples are heated up to 1,000 °C at Ar atmosphere, the weight losses for Graphite, GO, and *l*-GFs are observed to be 4.9%, 41.4%, and 100.0%, respectively.

S2.7. SEM images of Rubber composite

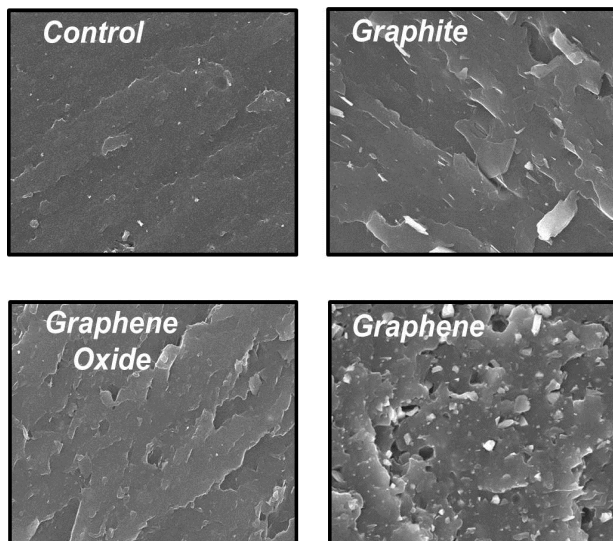


Figure S2.7. SEM image of fracture surfaces of the Rubber composites at 5 phr.

Figure S2.7 shows SEM images of the Control/SBR, Graphite/SBR, GO/SBR and *l*-GFs/SBR. The *l*-GFs/SBR observes rougher fractured surface ascribed to the surface modification of the *l*-GFs leading to stronger interfacial adhesion between the functionalized *l*-GFs and SBR matrix and preventing the motion of the SBR segmental chains. These results suggest that the *l*-GFs have a great reinforcing effect on SBR matrix with respect to few loadings because of increased physical/chemical interaction between *l*-GFs and Rubber.

Table S1. Formation of the Rubber composites

phr					
STEP	Materials	Control/SBR	Graphite/SBR	GO/SBR	<i>l</i> -GFs/SBR
STEP 1	SBR Latex	20	20	20	20
	Graphite	-	5	-	-
	Graphene Oxide (GO)	-	-	5	-
	Graphene (<i>l</i> -GFs)	-	-	-	5
STEP2	SBR	80	80	80	80
	Carbon Black	50	50	50	50
	Stearic Acid	1	1	1	1
	Sulfur	1.75	1.75	1.75	1.75
	TBBS	1	1	1	1

Table S2. Atomic ratios of the elements in Graphite, GO, and *l*-GFs analyzed with XPS

Element	C [at %]	O [at %]
Graphite	97.2	2.8
GO	68.7	31.8
<i>l</i> -GFs	88.8	11.2

Table S3. Curing properties of Rubber composites

	Control/SBR	Graphite/SBR	Graphene oxide/SBR	Graphene/SBR
T_{40} (min)	11.9	7.9	8.3	5.5
T_{90} (min)	14.8	10.1	11.1	8.2
Min Torque (M_L , dNm)	17.6	18.1	17.2	19.1
Max Torque (M_H , dNm)	34.8	36.0	35.8	39.9
Δ Torque	17.2	17.9	18.6	20.8

REFERENCES

- [1] M. Hirata, T. Gotou, S. Horiuchi, M. Fujiwara, M. Ohba, *Carbon* **2004**, 42, 2929.
- [2] D. X. Yang, F. Y. Kang and Y. P. Zheng, *Carbon Tech.*, **2000**, 2, 6.